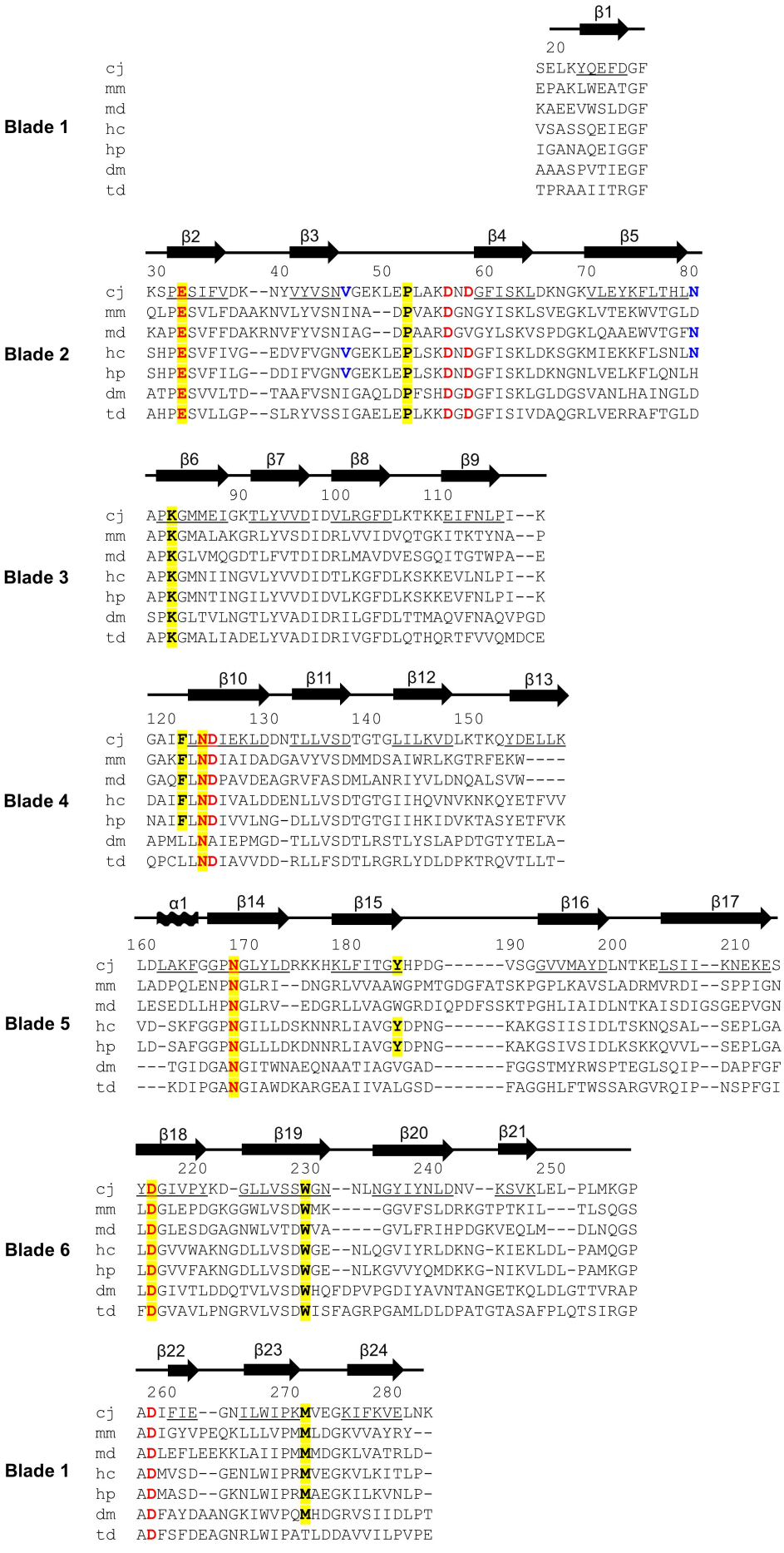

Supplementary Figure S1. Amino acid sequence alignment of CJ1041C (cj) and its orthologs (*Magnetospirillum moscoviense*, mm; *Mesorhizobium delmotii*, md; *Helicobacter canadensis*, hc; *Helicobacter pullorum*, hp; *Donghicola mangrovi*, dm; *Thioclava dalianensis*, td). The CJ1041C residues that coordinate Ca^{2+} ions using side chains and main chains are colored red and blue, respectively. The glycerol-binding residues of CJ1041C are highlighted by a yellow background. Identical residues in orthologs are highlighted or colored as shown for CJ1041C. The secondary structural elements of CJ1041C are indicated by arrows (β-strands) and a wave (α-helix) above the CJ1041C sequence.

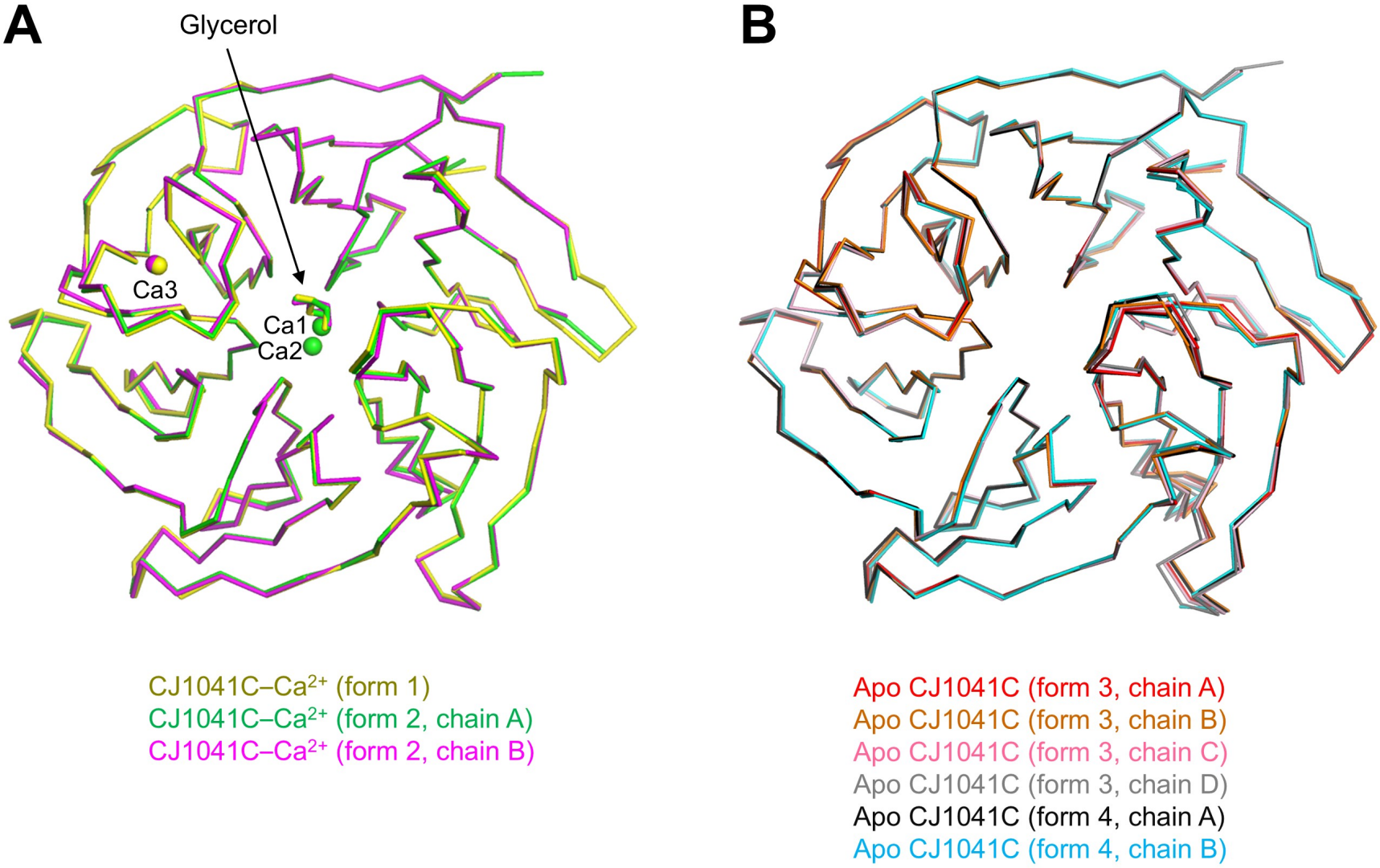

Supplementary Figure S2. Similar structures of the CJ1041C chains from crystal forms 1–4.
(A) Similar structures of the CJ1041C chains from CJ1041C–Ca^{2+} crystal forms 1 (yellow) and 2 (chain A, green; chain B, magenta). The CJ1041C structures are shown as Cα traces. Three Ca^{2+} ions (Ca1, Ca2, and Ca3) and a glycerol molecule from each CJ1041C structure are represented by spheres and sticks, respectively.
(B) Similar structures of the CJ1041C chains from apo CJ1041C crystal forms 3 (chain A, red; chain B, orange; chain C, pink; chain D, gray) and 4 (chain A, black; chain B, cyan).

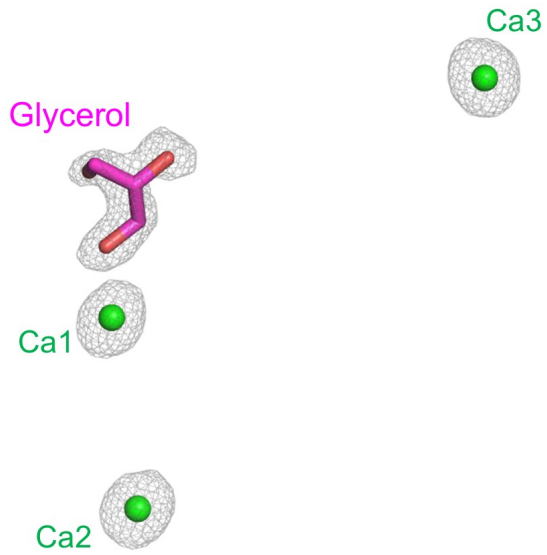

Supplementary Figure S3. F_o–F_c omit map (3σ level, gray wires) of the Ca^{2+} ions (green spheres) and glycerol molecule (magenta sticks) in the CJ1041C–Ca^{2+} structure.

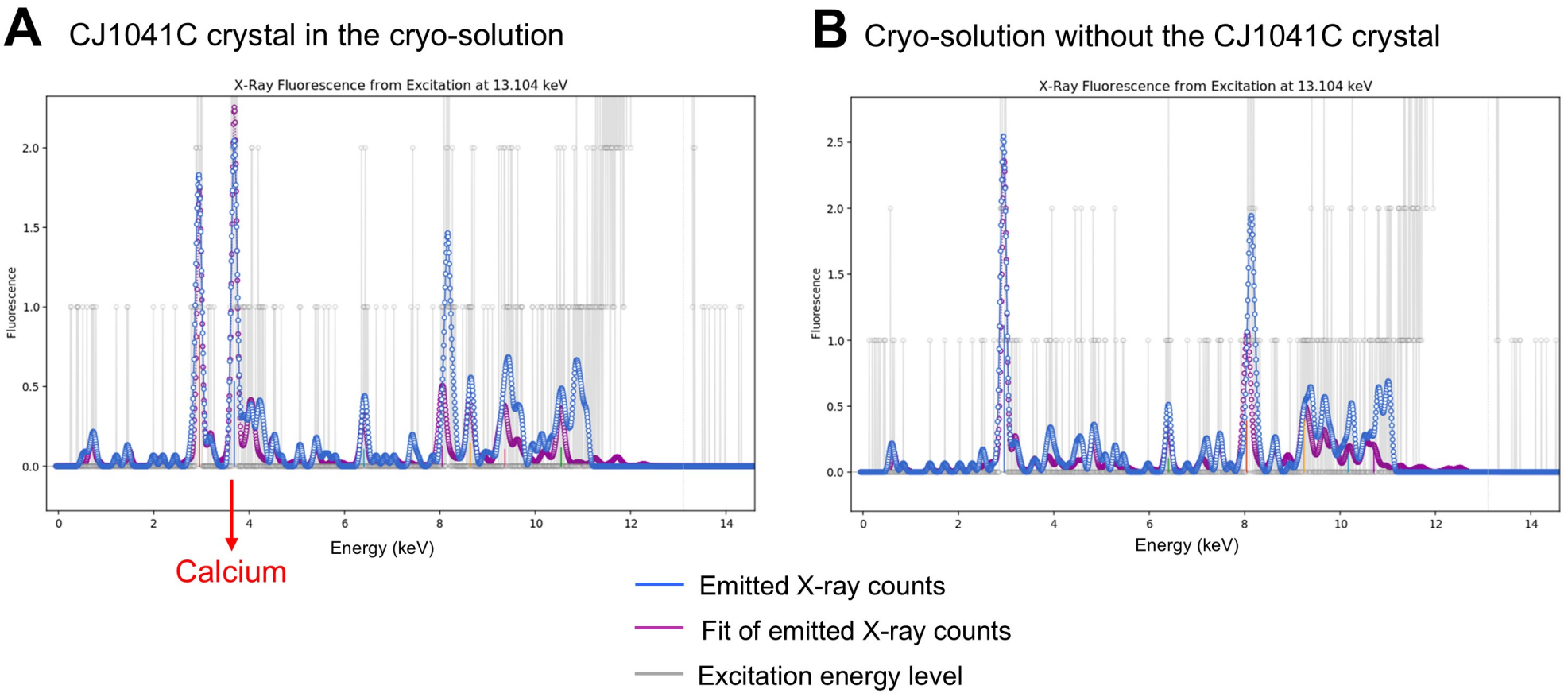

Supplementary Figure S4. X-ray fluorescence analysis to identify metal ions in the CJ1041C crystal. Emitted X-ray counts and their fits are shown in light blue and purple, respectively. X-ray fluorescence experiments were performed using X-rays with an excitation energy of ~13.1 keV. The excitation energy levels are shown in gray only over the displayed range (0–~3). The excitation energy level corresponding to 13.1 keV lies beyond this range (>60) and is therefore not shown.

(A) X-ray fluorescence spectrum of the CJ1041C crystal in the cryo-solution. A fluorescence peak corresponding to calcium is observed (red arrow).

(B) X-ray fluorescence spectrum of the cryo-solution without the CJ1041C crystal. No fluorescence peak corresponding to calcium is observed.

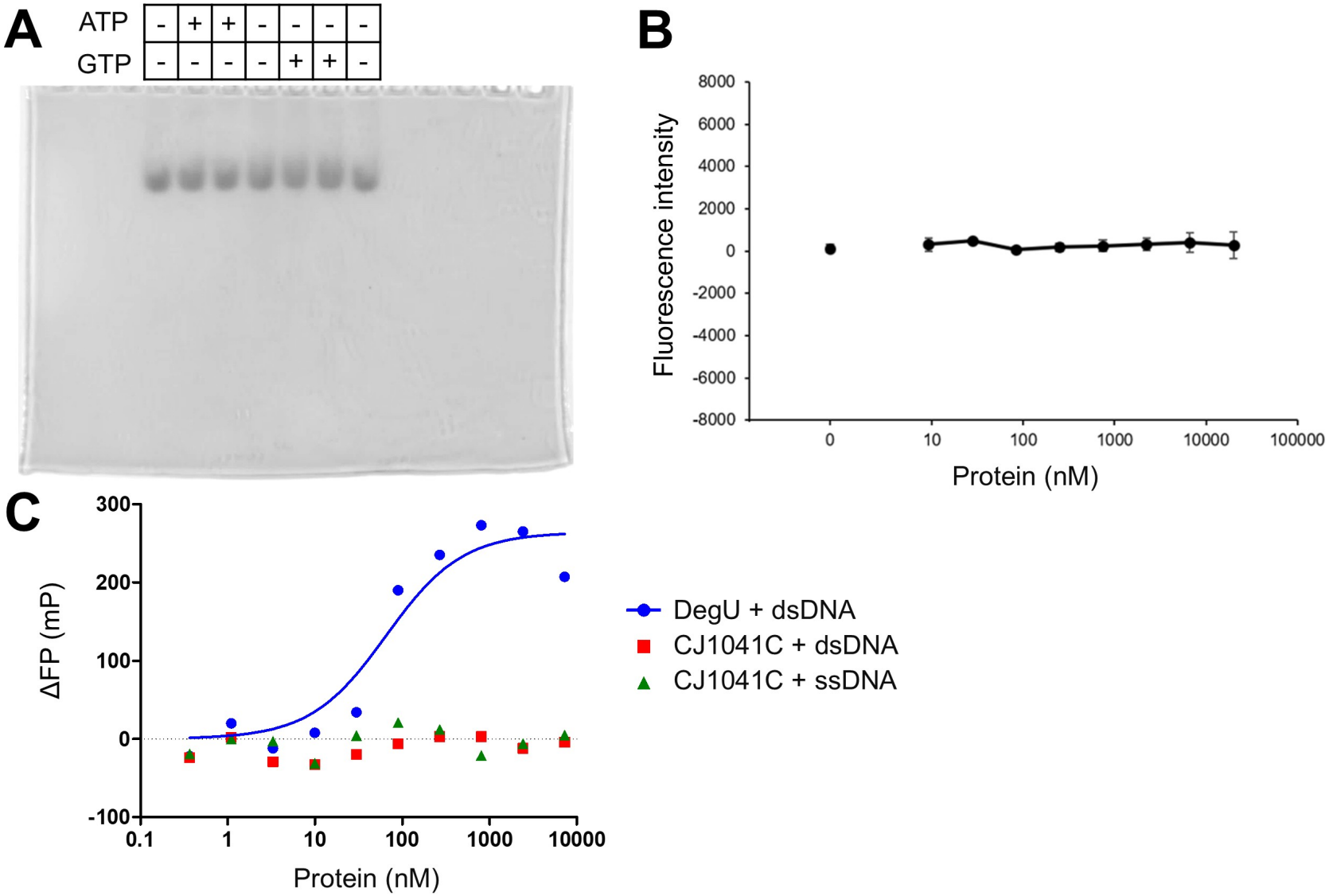

Supplementary Figure S5. No detectable interaction of CJ1041C with ATP, GTP, or DNA.

(A) Native PAGE analysis of CJ1041C in the absence and presence of 5 mM ATP and GTP. The results are representative of three independent experiments.

(B) Fluorescence assay (excitation wavelength, 350 nm; emission wavelength, 450 nm) assessing the interaction of CJ1041C with MANT-GTP in the presence of 10 mM Ca^{2+} and 10 mM Mg^{2+}. No significant change in fluorescence was observed. Data are presented as the mean ± SD (n = 4).

(C) Fluorescence polarization (FP) assay assessing the interaction of CJ1041C with dsDNA and ssDNA. CJ1041C showed no detectable interaction with either dsDNA or ssDNA, whereas the positive control protein DegU exhibited a strong interaction signal with dsDNA[29]. The results are representative of at least three independent experiments.

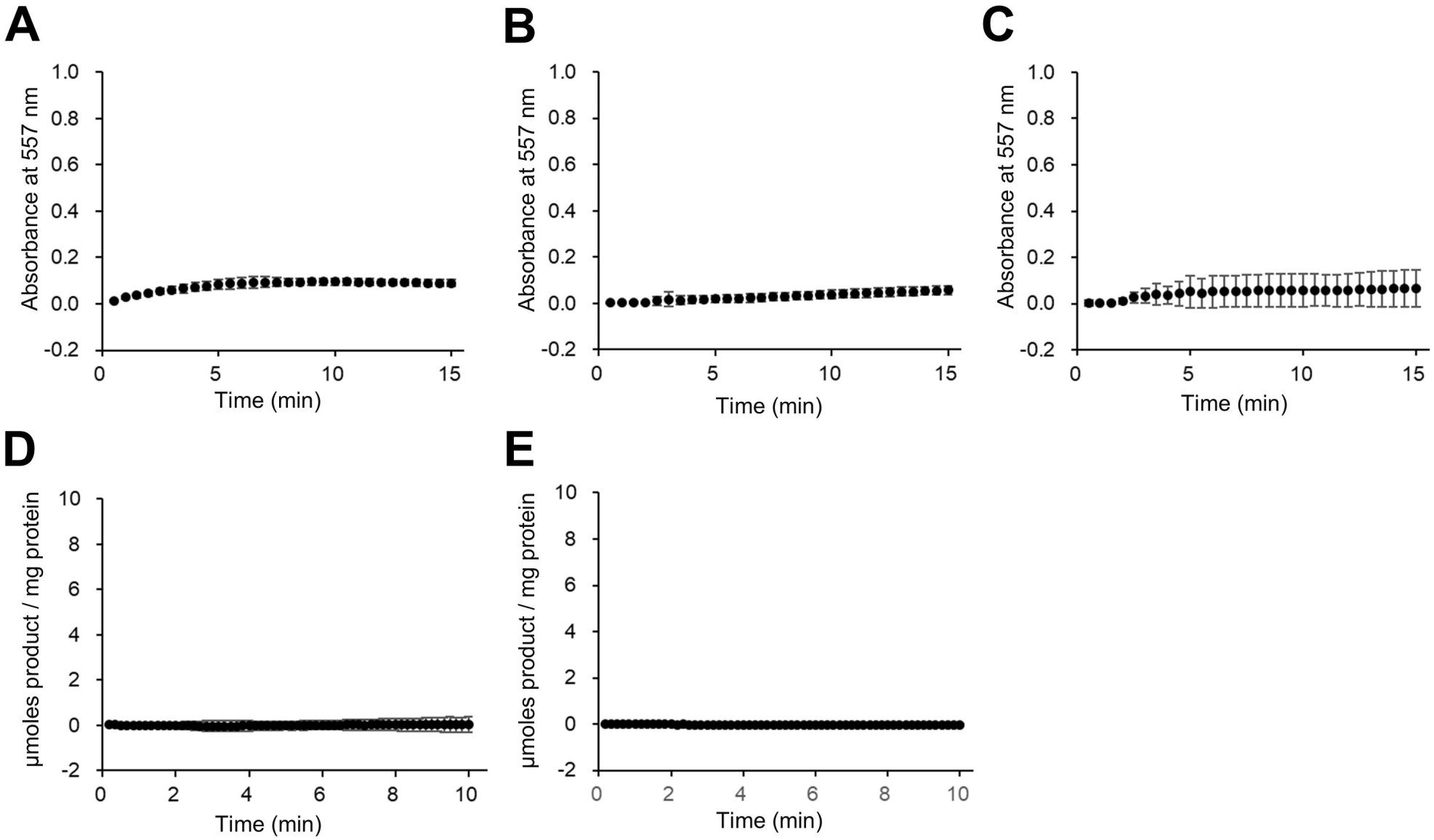

Supplementary Figure S6. Absence of hydrolytic activities of CJ1041C toward D-glucono-δ-lactone, L-gulonic acid γ-lactone, γ-valerolactone, dihydrocoumarin, and phenyl acetate.

(A–C) Analysis of the lactonase activity of CJ1041C toward D-glucono-δ-lactone (A), L-gulonic acid γ-lactone (B), and γ-valerolactone (C) at pH 7.5. A decrease in the absorbance at 557 nm indicates positive lactonase activity. The data are shown as the mean ± SD (n = 5 for D-glucono-δ-lactone and L-gulonic acid γ-lactone; n = 3 for γ-valerolactone).

(D) Analysis of the lactonase activity of CJ1041C toward dihydrocoumarin at pH 8.0. The data are shown as the mean ± SD (n = 5).

(E) Analysis of the arylesterase activity of CJ1041C toward phenyl acetate at pH 8.0. The data are shown as the mean ± SD (n = 7).

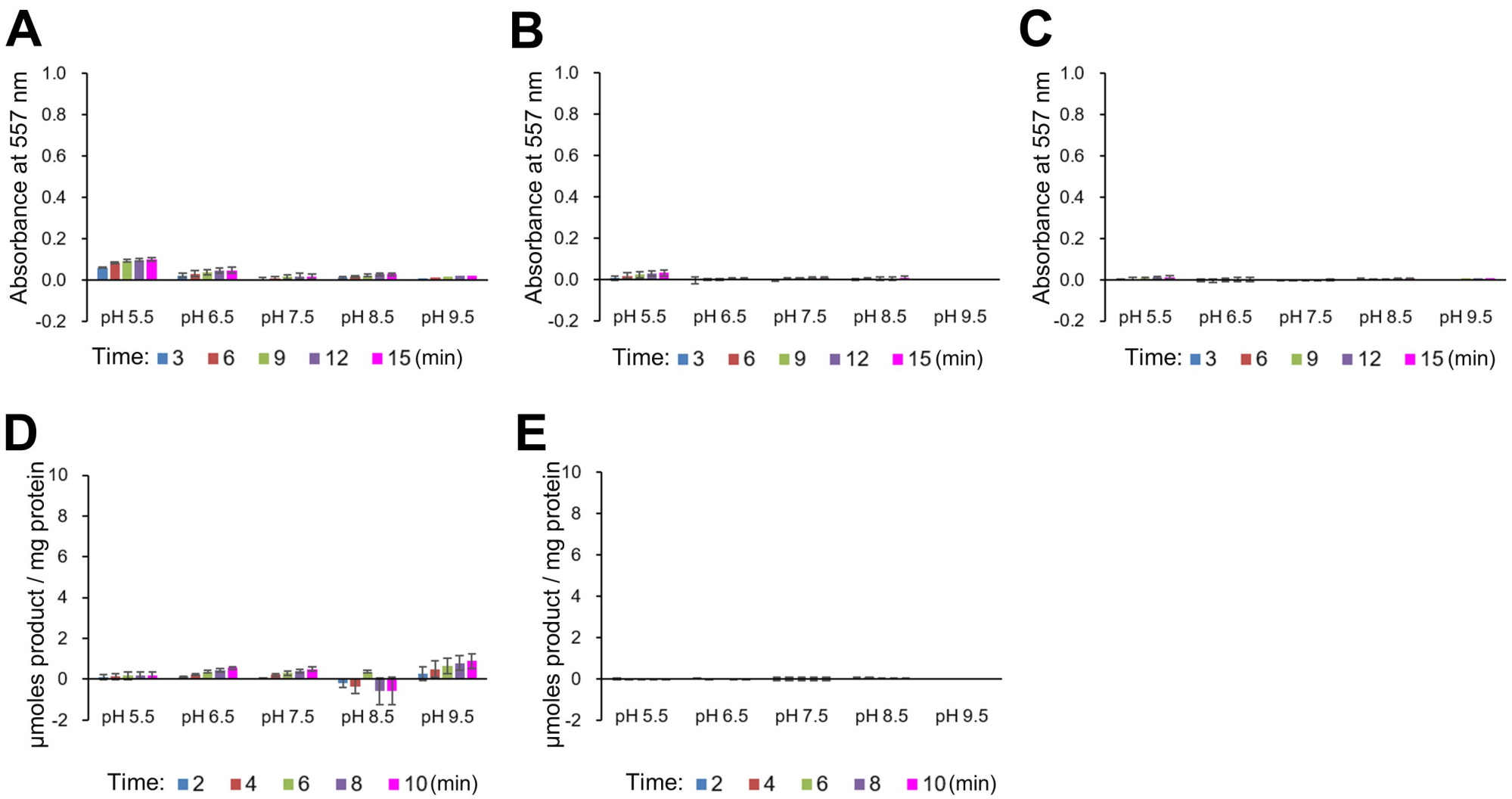

Supplementary Figure S7. Negligible hydrolytic activities of CJ1041C toward D-glucono-δ-lactone (A), L-gulonic acid γ-lactone (B), γ-valerolactone (C), dihydrocoumarin (D), and phenyl acetate (E) at pH 5.5, 6.5, 7.5, 8.5, and 9.5. The data are presented as the mean ± SD (n = 3).

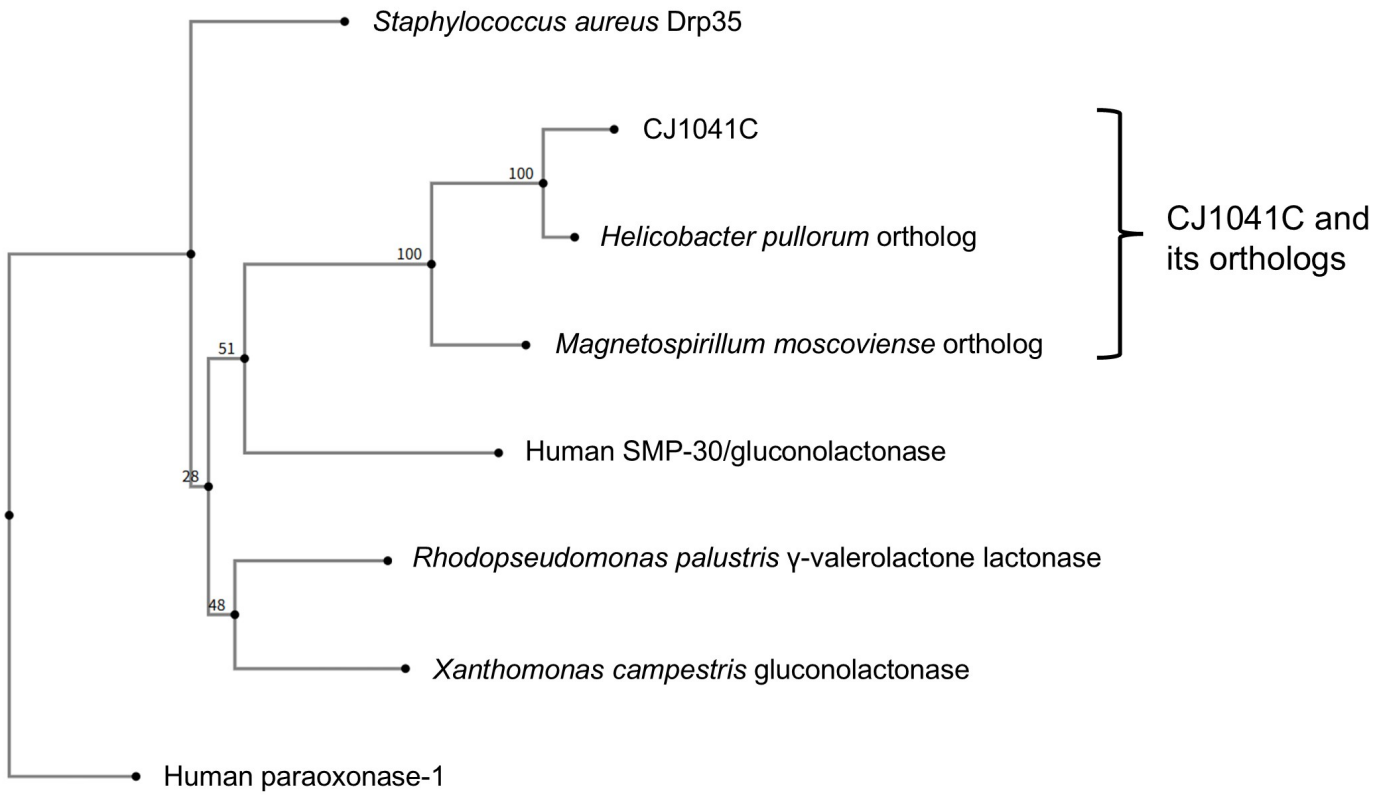

Supplementary Figure S8. Phylogenetic tree of CJ1041C, its orthologs, and β-propeller lactonases. Phylogenetic analysis was performed via the neighbor-joining method using the MAFFT server (https://mafft.cbrc.jp). A bootstrap value is shown as a percentage for each phylogenetic node. CJ1041C clusters tightly with its orthologs with strong bootstrap support (100%), whereas its grouping with structurally characterized β-propeller lactonases is poorly supported, with low bootstrap values.

Supplementary Table S1. Crystallographic statistics of the CJ1041C–Ca^{2+} structure.

	CJ1041C–Ca^{2+} form 1	CJ1041C–Ca^{2+} form 2
Data collection		
Space group	$P2_12_12_1$	P1
Cell parameters	a = 46.40 Å	a = 45.44 Å
	b = 60.63 Å	b = 46.15 Å
	c = 91.73 Å	a = 66.71 Å
	α = 90°	α = 87.38°
	β = 90°	β = 71.02°
	γ = 90°	γ = 81.71°
Wavelength (Å)	0.9793	0.9793
Resolution (Å)	30.00–1.50	30.00–2.00
Highest resolution (Å)	1.53–1.50	2.03–2.00
No. unique reflections	42,021 (1,907) [a]	33,428 (1,597) [a]
R_{merge} [b]	0.139 (0.662) [a]	0.105 (0.584) [a]
R_{meas} [c]	0.153 (0.733) [a]	0.125 (0.715) [a]
R_{pim} [d]	0.062 (0.309) [a]	0.067 (0.407) [a]
$CC_{1/2}$ [e]	0.986 (0.749) [a]	0.988 (0.710) [a]
I/σ(I)	16.9 (1.9) [a]	9.0 (1.2) [a]
Completeness (%)	99.3 (92.6) [a]	97.8 (94.6) [a]
Redundancy	5.9 (5.1) [a]	3.3 (2.7) [a]
Refinement		
Resolution (Å)	30.00–1.50	30.00–2.00
No. of reflections (work)	39,799	31,750
No. of reflections (test)	2,071	1,666
R_{work} (%) [f]	17.1	16.0
R_{free} (%) [g]	19.9	20.1
No. atoms		
Protein	2,073	4,059
Ligands	9	18
Water	211	188
Average B-value ($Å^2$)	18.2	25.4
RMSD bonds (Å)	0.006	0.008
RMSD angles (°)	0.907	0.971
Ramachandran [h] (favored)	93.9%	94.8%
(outliers)	0.0%	0.0%

[a] Numbers in parenthesis were calculated from data of the highest resolution shell.
[b] $R_{merge} = \Sigma_{hkl}\Sigma_i \mid I_i(hkl) - \langle I(hkl)\rangle \mid / \Sigma_{hkl}\Sigma_i I_i(hkl)$
[c] $R_{meas} = \Sigma_{hkl}\{N(hkl)/[N(hkl) - 1]\}^{1/2} \Sigma_i \mid I_i(hkl) - \langle I(hkl)\rangle \mid / \Sigma_{hkl}\Sigma_i I_i(hkl)$
[d] $R_{pim} = \Sigma_{hkl}\{1/[N(hkl) - 1]\}^{1/2} \Sigma_i \mid I_i(hkl) - \langle I(hkl)\rangle \mid / \Sigma_{hkl}\Sigma_i I_i(hkl)$
[e] Correlation coefficient between intensities from random half-data sets.
[f] $R_{work} = \Sigma \mid |F_{obs}|-|F_{calc}| \mid / \Sigma|F_{obs}|$, where F_{calc} and F_{obs} are the calculated and observed structure factor amplitudes, respectively.
[g] R_{free} = as for R_{work}, except that 5% of the total reflections were selected at random and omitted from refinement.
[h] Calculated using MolProbity (http://molprobity.biochem.duke.edu).

Supplementary Table S2. Crystallographic statistics of the CJ1041C structure in the apo form.

	CJ1041C form 3	CJ1041C form 4
Data collection		
Space group	P2	C2
Cell parameters	a = 80.76 Å	a = 141.55 Å
	b = 56.40 Å	b = 56.15 Å
	c = 121.02 Å	a = 80.55 Å
	α = 90°	α = 90°
	β = 97.54°	β = 120.06°
	γ = 90°	γ = 90°
Wavelength (Å)	0.9793	0.9794
Resolution (Å)	30.00–2.00	30.00–1.95
Highest resolution (Å)	2.03–2.00	1.98–1.95
No. unique reflections	70,660 (2,961) [a]	38,518 (1,557) [a]
R_{merge} [b]	0.083 (0.560) [a]	0.059 (0.458) [a]
R_{meas} [c]	0.100 (0.672) [a]	0.071 (0.546) [a]
R_{pim} [d]	0.054 (0.367) [a]	0.038 (0.294) [a]
$CC_{1/2}$ [e]	0.990 (0.694) [a]	0.997 (0.860) [a]
I/σ(I)	12.9 (1.2) [a]	14.1 (1.3) [a]
Completeness (%)	96.5 (81.2) [a]	96.8 (79.4) [a]
Redundancy	3.2 (2.8) [a]	3.2 (3.0) [a]
Refinement		
Resolution (Å)	30.00–2.00	30.00–1.95
No. of reflections (work)	67,072	36,622
No. of reflections (test)	3,555	1,871
R_{work} (%) [f]	18.7	21.8
R_{free} (%) [g]	22.6	25.7
No. atoms		
Protein	8,119	4,023
Water	246	131
Average B-value (Å^2)	41.5	45.2
RMSD bonds (Å)	0.007	0.008
RMSD angles (°)	0.975	1.021
Ramachandran [h] (favored)	94.6%	93.4%
(outliers)	0.0%	0.0%

[a] Numbers in parenthesis were calculated from data of the highest resolution shell.

[b] $R_{merge} = \Sigma_{hkl}\Sigma_i \mid I_i(hkl) - \langle I(hkl)\rangle \mid / \Sigma_{hkl}\Sigma_i I_i(hkl)$

[c] $R_{meas} = \Sigma_{hkl}\{N(hkl)/[N(hkl) - 1]\}^{1/2} \Sigma_i \mid I_i(hkl) - \langle I(hkl)\rangle \mid / \Sigma_{hkl}\Sigma_i I_i(hkl)$

[d] $R_{pim} = \Sigma_{hkl}\{1/[N(hkl) - 1]\}^{1/2} \Sigma_i \mid I_i(hkl) - \langle I(hkl)\rangle \mid / \Sigma_{hkl}\Sigma_i I_i(hkl)$

[e] Correlation coefficient between intensities from random half-data sets.

[f] $R_{work} = \Sigma \mid \mid F_{obs}\mid - \mid F_{calc}\mid \mid / \Sigma \mid F_{obs}\mid$, where F_{calc} and F_{obs} are the calculated and observed structure factor amplitudes, respectively.

[g] R_{free} = as for R_{work}, except that 5% of the total reflections were selected at random and omitted from refinement.

[h] Calculated using MolProbity (http://molprobity.biochem.duke.edu).